Chemical Science

EDGE ARTICLE

View Article Online
View Journal | View Issue

Cite this: *Chem. Sci.*, 2017, **8**, 2994

An efficient on-board metal-free nanocatalyst for controlled room temperature hydrogen production†

Saswati Santra,*[a] Debanjan Das,[a] Nirmalya Sankar Das[b] and Karuna Kar Nanda*[a]

Received 12th January 2017
Accepted 29th January 2017

DOI: 10.1039/c7sc00162b

rsc.li/chemical-science

Positively charged functionalized carbon nanodots (CNDs) with a variety of different effective surface areas (ESAs) are synthesized *via* a cheap and time effective microwave method and applied for the generation of hydrogen *via* hydrolysis of sodium borohydride. To the best of our knowledge, this is the first report of metal-free controlled hydrogen generation. Our observation is that a positively charged functional group is essential for the hydrolysis for hydrogen production, but the overall activity is found to be enhanced with the ESA. A maximum value of 1066 ml g^{-1} min^{-1} as the turnover frequency is obtained which is moderate in comparison to other catalysts. However, the optimum activation energy is found to be 22.01 kJ mol^{-1} which is comparable to well-known high cost materials like Pt and Ru. All of the samples showed good reusability and 100% conversion even after the 10th cycle. The effect of H^+ and OH^- is also studied to control the on-board and on-demand hydrogen production ("on–off switching"). It is observed that H_2 production decreases inversely with NaOH concentration and ceases completely when 10^{-1} M NaOH is added. With the addition of HCl, H_2 production can be initiated again, which confirms the on/off control over production.

Introduction

Finding efficient and clean alternative energy sources is one of the prime concerns for modern research due to the depletion of fossil-fuel reserves and increase in environmental pollution. In this regard, hydrogen is a potential alternative to traditional fuels like, coal, oil, natural gas, *etc.*[1–3] It can perform more efficiently than gasoline in inner combustion systems and its better compression ratio is an advantage.[4,5] Moreover, no pollutants like carbon monoxide, odor, or soot are produced during the combustion process. Hydrogen is also used as fuel in proton exchange membrane (PEM) fuel cells, and this kind of fuel cell offers zero/low emissions.[6,7] Due to their high performance, these cells are proven to be substitutes for the internal-combustion engine in transport systems and residential power production.[8–11] However, the prime source of hydrogen production is hydrocarbons and as a result carbon monoxide is also produced simultaneously as a by-product that affects the purity of the produced hydrogen, and hence, the performance of PEM fuel cells. Moreover, due to a very low volumetric energy density, storage of hydrogen requires highly pressurized cylinders resulting in disadvantages like heavy weight, space occupancy, safety concerns, *etc.* In order to use PEM fuel cells in transport systems, 'on-board' hydrogen production or light weight hydrogen storage methods are required and are of paramount importance. Some metal hydrides like $LaNi_5H_6$ have been studied as hydrogen storage materials. Nevertheless, they have lots of drawbacks such as having too low a gravimetric storage capacity (1–2 wt%), high cost, high temperature requirements for generating hydrogen, *etc.*[12] Above all, the major concerns are easy control, safety, high production rate and storage capability of hydrogen. In this regard, sodium borohydride ($NaBH_4$) has attracted much attention for its high hydrogen content of 10.8 wt%, environment-friendly nature and easy availability.[13–15] Schlesinger *et al.* reported that one molecule of $NaBH_4$ releases four hydrogen atoms and water soluble sodium metaborate ($NaBO_2$).[16] The chemical reaction follows the below chemical equation.

$$NaBH_4 + 2H_2O = 4H_2 + NaBO_2 + \text{heat (300 kJ)}$$

In this hydrolysis reaction, a catalyst plays an important role in controlling the hydrogen evolution at a practical rate. Precious metals and their composites like, Pt, Ru,[3,17,18] Pt–Ru,[19] graphene–Pt–Ni[20,21] *etc.* as well as some low cost metals and compounds *i.e.* nickel boride,[22,23] carbon supported Co,[24,25] cobalt boride[26,27] *etc.* have been exploited as catalyst in the hydrolysis of $NaBH_4$. A lot of studies have been carried out using

[a]*Materials Research Centre, Indian Institute of Science, Bangalore-560012, India. E-mail: santra.saswati@gmail.com; nanda@mrc.iisc.ernet.in*

[b]*Department of Basic Science and Humanities, Techno India – Batanagar, Kolkata 700141, India*

† Electronic supplementary information (ESI) available. See DOI: 10.1039/c7sc00162b

different dimensional carbon materials.[28–30] To the best of our knowledge, metal-free carbon nanostructures have not been exploited so far, though they are very stable, environment-friendly and cost-effective materials. In this paper, we have reported for the first time a metal-free catalyst for H_2 evolution using quasi zero-dimensional (0D) carbon nanodots (CNDs) and have studied in detail the catalytic activities by varying the surface area and the surface functionalities. We synthesize CNDs with varieties of different effective surface areas (ESAs) and positively charged functional groups at the surface *via* microwave treatment of citric acid (CA) monohydrate and urea. Negatively charged functional groups due to the presence of carboxyl groups on the surface are present when CA is treated with microwaves. The negatively charged functional group is futile for H_2 generation. However, the positively charged functional groups on CND surfaces, which are favorable for the hydrolysis, are realized when urea was added to CA. The CNDs are then applied for the generation of hydrogen *via* hydrolysis of sodium borohydride and our results indicate that positively charged functional groups are essential for the hydrolysis for hydrogen production, but the overall activity is found to be enhanced with the ESA. True activity, reusability and conversion of the as-synthesized CNDs have also been studied up to the 10^{th} cycle. For "on–off" switching of the H_2 production, pH dependent activity has also been examined and it was found that the activity has inverse relation with pH.

Experimental section

Synthesis

A simple, cheap, and time effective one-step, one-pot synthesis procedure was used to prepare the CNDs.[31] 1.4×10^{-2} M CA monohydrate and 5×10^{-2} M urea were mixed well *via* stirring for 10 min in 10 ml of deionized water to prepare a transparent solution at room temperature. This solution was kept in a domestic microwave oven and the reaction time varied from 2.5 to 4.5 min. As soon as the reaction was initiated, the solution started bubbling and the color changed from transparent to light orange to dark orange gradually. Finally a deep brown gel was obtained after natural cooling (Fig. S1†). Thereafter the samples were made soluble in deionized water and were purified in a centrifuge at 3200 rpm for 30 min to remove large or agglomerated particles. The final brown colored solutions were then collected for further analysis. Samples synthesized with a reaction time of 2.5, 3.5 and 4.5 min are labeled as sample A, B and C, respectively. The synthesis mechanism is discussed below (Scheme 1).

Characterizations

The as-synthesized samples were characterized using an X-ray diffractometer (XRD) using Bruker D8 Advance and WITec Raman system for phase confirmation. Fourier transform infrared spectroscopy (FTIR, Bruker 600) and X-ray photoelectron spectroscopy (XPS, AXIS ULTRA DLD) were used to study the bonding information and elemental analysis. The morphology was characterized using a JEOL transmission

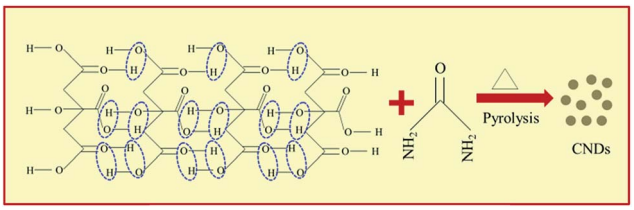

Scheme 1 Formation of CNDs from citric acid.

electron microscope (TEM) at 200 keV. For microscopic investigation, the samples with very low concentrations were first ultrasonicated in pure ethanol for 3 min and then dropped on Cu grids covered with a continuous carbon film. Zeta potential was studied using zeta potential analyzer (Brookhaven). A typical three-electrode cell attached to a CHI750E workstation was used for the electrochemical measurements. A saturated calomel electrode (SCE) and Pt wire were used as the reference and counter electrode, respectively. A commercially available glassy carbon electrode (GCE, 3 mm diameter, 0.07 cm^2) was used as the working electrode. In order to prepare the electrode, 2 mg of catalyst and 500 μl of ethanol were used to prepare the primary solution. Then 20 μl of 5 wt% Nafion© 117 solution was added to this as binder and the solution was sonicated for 30 min to obtain the final catalyst ink. 15 μl of ink was drop-casted onto the GCE followed by air-drying to obtain the catalyst loading of ~0.75 mg cm^{-2}. 1 M KOH solution (pH = 14, purged with N_2 gas for 30 min at room temperature) was used as electrochemical solvent.

Hydrogen generation *via* hydrolysis of $NaBH_4$

The water displacement method was used to determine the catalytic activities of the as-synthesized CNDs for the hydrolysis of $NaBH_4$. A thermostatic bath was used to maintain the temperature of the reaction flask. Another flask filled up with water was connected to the reaction flask to measure the volume of H_2 gas produced by the hydrolysis. The reaction flask was also equipped with a burette to control the water flow and volume used for hydrolysis. Before the reaction started a certain amount of $NaBH_4$ (2 g) and catalyst (0.05 g) was measured precisely and added together into the reaction flask which was air tight. Then 50 ml of water was added from the burette while the stirring was on. After all of the water was added (30 s), the measurement of H_2 evolution with respect to time was started *via* water displacement.

Results and discussion

CNDs can be obtained from CA *via* H-bonding assisted self-assembly followed by pyrolysis during microwave treatment (Scheme 1). CNDs with negatively charged carboxyl (>COO^-, >C=O) functional groups are obtained when only CA is microwave-treated. However, CNDs with positively charged (NH_4^+) functional groups are obtained when urea was added along with CA and treated with microwaves.[32] Grafting the CNDs with positive functional groups is crucial since it

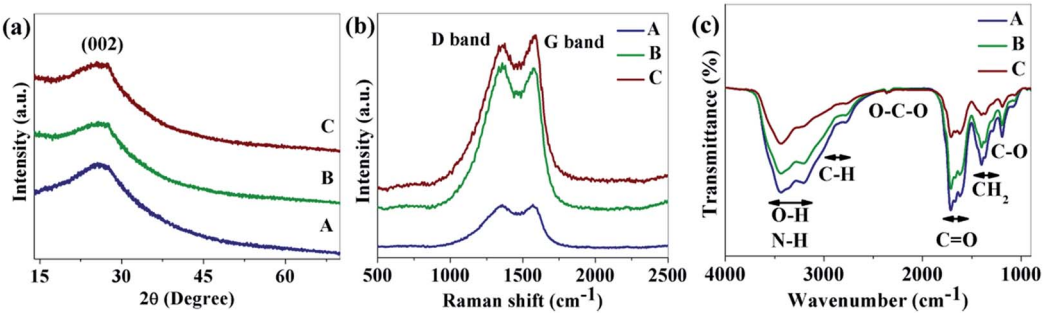

Fig. 1 (a) XRD patterns; (b) Raman spectra; and (c) FTIR spectra of samples A, B and C.

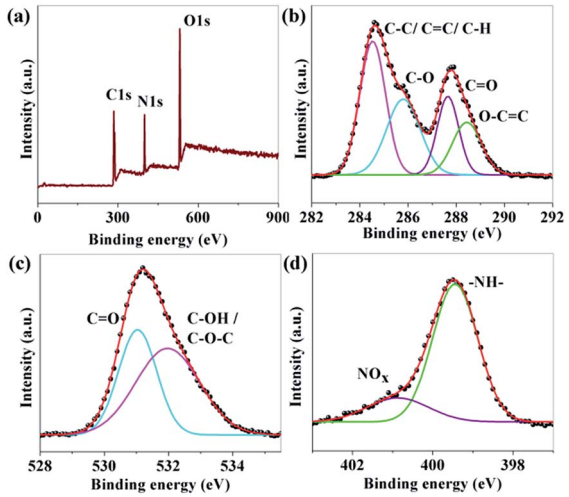

Fig. 2 (a) XPS survey scan; and (b–d) XPS high resolution survey scan of the C1s, O1s and N1s regions of sample B respectively.

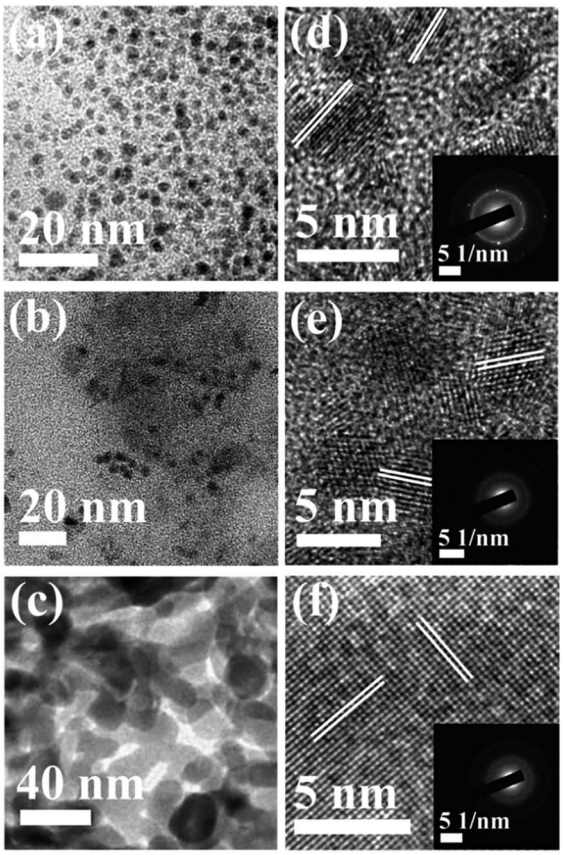

Fig. 3 (a–c) TEM images; and (d–f) lattice images of samples A, B and C, respectively. Insets show the corresponding SAED patterns.

facilitates the borohydride ion (BH_4^-) onto the surface of the CNDs for hydrogen generation, which is futile in the presence of negatively charged CNDs. Urea undergoes hydrolysis with the release of CO_2 as follows:

$$NH_2–CO–NH_2 + 2H^+ + H_2O \rightarrow 2NH_4^+ + CO_2$$

The NH_4^+ ion so formed is then drawn to the surface of the CNDs due to electrostatic attraction from the $–COO^-$ groups already present on the CNDs' surface.

Fig. 1a shows the XRD patterns of the as-synthesized CNDs. As shown in the figure, a broad peak near 26.3° was found for all of the CNDs which corresponds the (002) plane of graphitic carbon.[33] Raman spectra of the as-prepared CNDs are shown in Fig. 1b. The peak around 1360 cm^{-1} (D band) corresponds to the vibrations of carbon atoms with dangling bonds at the edge of the plane of disordered graphite or glassy carbon. The G band at 1576 cm^{-1} is associated with the E_{2g} mode of the graphite which is related to the vibration of sp^2-bonded carbon atoms in a hexagonal lattice.[34]

FTIR was used to detect the surface functional groups of the CNDs (Fig. 1c). Broad absorption bands at 3100–3500 cm^{-1} are assigned to ν(O–H) and N–H, 2800–3100 cm^{-1} is for the stretching mode of C–H, 2350 cm^{-1} is labeled as O–C–O and 1600–1770 cm^{-1}, 1350–1460 cm^{-1} and 1190 cm^{-1} are for ν(C=O), $\delta(CH_2)$ and the stretching mode of C–O respectively.[31,35–37]

The composition and elemental analysis of the as-synthesized CNDs were characterized using XPS. The XPS spectrum of sample B (Fig. 2a) depicts three peaks at 284.6, 400.0, and 530.5 eV, which confirms the presence of C, N, and O, respectively. In the high resolution spectrum of C1s (Fig. 2b), the peaks at 284.6, 285.8, 287.7 and 288.4 eV are assigned to be C–C/C=C/C–H, C–O, C=O and O–C=O, respectively.[38–41]

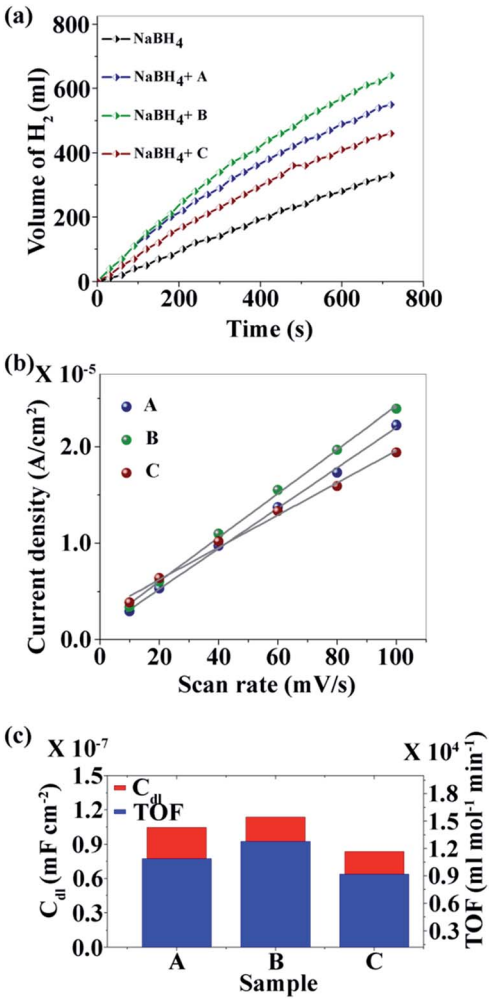

Fig. 4 (a) Kinetics study; (b) linear fit of the differences in current density variation at a potential of 0.16 V *vs.* scan rate for the estimation of C_{dl}; and (c) relationship between C_{dl} and TOF.

Table 1 Comparison of TOFs of metal-free CNDs with other metal catalysts

Material	TOF (ml g^{-1} min^{-1})	Reference
Co	539.6	47
Ni	1803	48
Co–B	1268	49
Poly(vinylidene fluoride)-Ni	55.6	50
CND	1066	This work

The O1s spectrum (Fig. 2c) shows peaks at 531.0 and 532.1 eV which are associated with C=O and C–OH/C–O–C, respectively.[39,40] A broad peak from 403 to 409 eV related to N1s are shown in Fig. 2d. The de-convoluted peaks at 399.4 and 400.9 eV are assigned to –NH– and N–O_x respectively.[41–45] No C–N peak was found in the XPS data which confirms that nitrogen is only attached to the surface of the CNDs. The percentage amount of nitrogen was found to be 9.89, 15.19 and 12.61 for A, B and C, respectively.

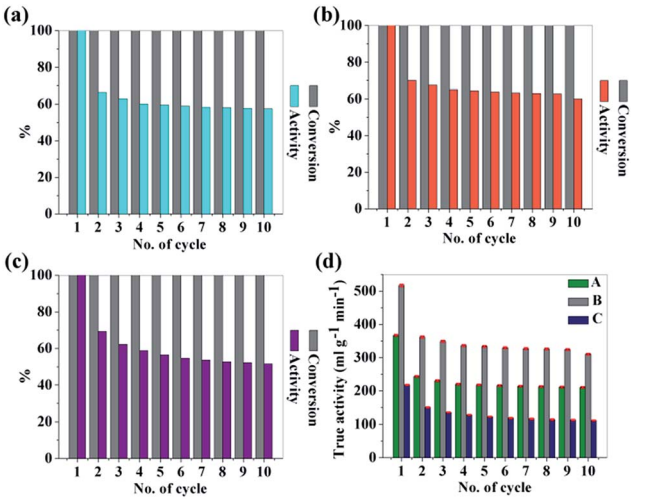

Fig. 5 (a–c) Reuse of sample A, B and C to study the conversion and activity as catalyst in H_2 production *via* the hydrolysis of $NaBH_4$; (d) true activity values for each sample up to 10 cycles.

Fig. 3a–c show the TEM images of the CNDs which reveal the average diameters as ~2.5, ~3.5 and ~15.6 nm for samples A, B and C, respectively. The high resolution TEM (HRTEM) images (Fig. 3d–f) reveal the crystalline nature with in-plane lattice spacing of 0.24 and 0.33 nm, corresponding to the (1120) and (002) planes, respectively, which also confirms the proper phase formation of graphitic carbon.[46] The insets show selected area electron diffraction (SAED) patterns that also endorse the nanocrystalline nature of the same. The cumulative volumes of hydrogen generation at room temperature over time for the hydrolysis reaction of $NaBH_4$ using various catalysts and without catalysts are presented in Fig. 4a. For all of the cases, H_2 generation started as soon as water was added with $NaBH_4$ and all of the CNDs showed higher H_2 evolution rates as compared to the non-catalytic reaction. To quantify the catalytic activity, the turnover frequency (TOF) was estimated using the following equation for all of the CNDs.

$$\mathrm{TOF} = \frac{\text{volume of hydrogen generated}}{\text{weight of catalyst used } X \text{ time}}$$

It was found that sample B showed the highest hydrolysis activity with respect to all of the other samples. The TOFs of different metal catalysts are compared with sample B (the best sample in our case) in Table 1. It can be noted that metal-free CNDs can compete with other metallic catalysts.

XPS analysis reveals the presence of electron withdrawing –NH– species on the surface of CNDs in the order of B > C > A and the zeta potential was recorded for each sample *in operando*, and was found to be 12.92, 23.10 and 15.15 mV respectively for sample A, B and C. Thus it is expected that the rate of hydrolysis of BH_4^- would follow the same order by virtue of the electrostatic interactions.

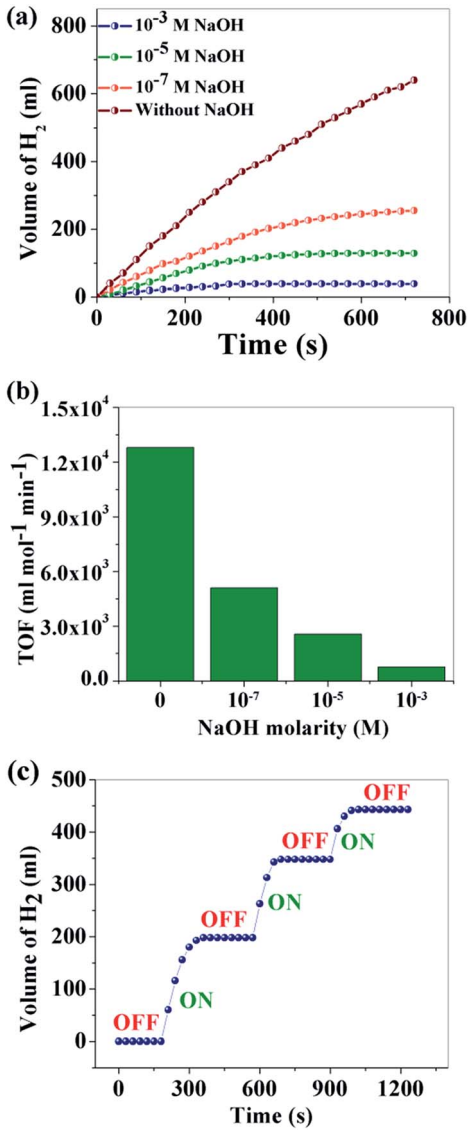

Fig. 6 (a) Effect of NaOH concentration on H_2 generation; (b) TOF at different concentrations of NaOH; (c) "on–off" control of H_2 production.

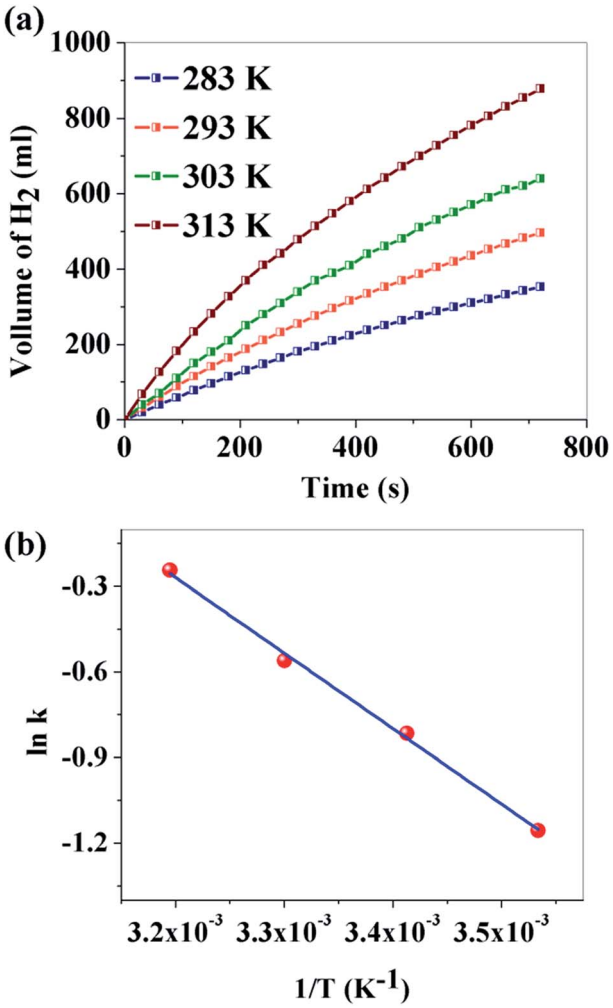

Fig. 7 (a) Effect of reaction temperature in H_2 generation; (b) corresponding Arrhenius plot.

However, the observed hydrolysis trend follows the order of B > A > C. To explain this apparent anomaly the effective surface area (ESA) of the catalysts, a crucial factor that can influence the catalytic activity, was taken into account. The double-layer capacitance (C_{dl}) which is linearly proportional to ESA, is determined from the cyclic voltammogram (CV).[51] CV studies were carried out at various scan rates (10, 20, 40, 60, 80 and 100 mV s^{-1}) in the voltage range of −0.25 to 0.05 V (Fig. S5a–c†). The differences in current density ($\Delta J = J_a - J_c$) at a potential of 0.16 V with respect to the scan rate are plotted and fitted with linear relation (Fig. 4b). The value of C_{dl} is half of the slope and it is found that $C_{dlB} > C_{dlA} > C_{dlC}$ which is directly related to the ESA of the samples. The TOF and ESA are compared in Fig. 4c. It can be noted that the catalytic activity of the CNDs follows the same trend as the ESA.

To investigate the reusability of the as-synthesized CNDs as catalyst, hydrolysis experiments were consecutively carried out for 10 times in the same reaction media by just adding the same amount of $NaBH_4$ for each cycle. The conversion was 100% but the catalytic activity degraded for each cycle. The drop in the catalytic activity of the CNDs may be due to by-product formation during hydrolysis. However the CNDs showed good reusability and after the 10th cycle the activities of samples A, B and C are found to be ∼57%, ∼60% and ∼52% respectively. The recorded data are depicted in Fig. 5a–c.

Self-hydrolysis occurs when water is added to $NaBH_4$. So to figure out the actual effectiveness of the CNDs as efficient catalysts, true activity values are significant to figure out. For this, self-hydrolysis of $NaBH_4$ was studied for 10 cycles and it remained almost the same for all of the cycles (550 ml g^{-1} min^{-1}). With this data, true activities for all of the samples are also calculated using the following equation[52] and are depicted in Fig. 5d.

True activity = activity over catalyst − activity without catalyst

Table 2 Comparison of the activation energy of CND with other reported materials

Material	Type of reaction	Activation energy (kJ mol^{-1})	Reference
Pt/CNT	Hydrolysis	38	18
Ru	Hydrolysis	47	55
Nickel boride	Hydrolysis	38	56
Ru nanocluster	Hydrolysis	28.51	57
Ni-nanogel	Hydrolysis	50.96	58
$CuFe_2O_4$/RGO	Hydrolysis	33.95	59
p(TAEA-*co*-GDE) microgels	Methanolysis	30.37	60
$p(2\text{-VP})^{2+}$C6 particles	Methanolysis	20.84	61
Phosphorus modified boehmite	Methanolysis	21.6	62
$p(4\text{-VP})^{2+}$C6	Methanolysis	13.78	63
Poly(ethylene imine) microgel	Methanolysis	23.7	64
CND	Hydrolysis	22.01	This work

Self-hydrolysis of $NaBH_4$ follows the mechanism stated below:[53]

Step 1:

$$NaBH_{4(s)} \leftrightarrow Na_{(aq)}^{+} + BH_{4(aq)}^{-}$$

Step 2:

$$BH_{4(aq)}^{-} + H_{(aq)}^{+} \leftrightarrow BH_{3(aq)} + H_{2(g)}$$

Step 3:

$$BH_{3(aq)} + 3H_2O_{(l)} \rightarrow B(OH)_{3(aq)} + 3H_{2(g)}$$

Step 4:

$$B(OH)_{3(aq)} + H_2O_{(l)} \leftrightarrow B(OH)_{4(aq)}^{-} + H_{(aq)}^{+}$$

Step 5:

$$4B(OH)_{4(aq)}^{-} + 2H_{(aq)}^{+} \leftrightarrow B_4O_{7(aq)}^{2-} + 9H_2O_{(l)}$$

Control of the "on–off" conditions for H_2 production is crucial for portable applications. It can be noted from step 2 that the production of protons controls the total process. If the proton production can be controlled, the H_2 production rate can easily be controlled. Basic media is a very well-known source OH^- which can control H^+ production. To study the effect of basic solution on the hydrolysis of $NaBH_4$, NaOH solutions of different concentrations (10^{-1} M, 10^{-3} M, 10^{-5} M and 10^{-7} M) were used and the catalytic activity was examined. As expected, H_2 production decreased gradually with the increase of NaOH concentration (Fig. 6a). The TOFs for different concentrations of NaOH are compared in Fig. 6b. The volume of H_2 production in 720 s is 640 ml with only water while H_2 production ceased completely for a 10^{-1} M NaOH concentration (no associated figure). Additionally, herein for the first time, we demonstrated that the H_2 production *via* $NaBH_4$ hydrolysis can be reversibly turned "off" and "on", which can be of great practical importance for on-site and on-demand hydrogen usage. The "on–off" control of hydrogen production (Fig. 6c) is achieved *via* addition of an equimolar amount of HCl and NaOH. Here HCl is used as a source of H^+ which plays a positive role in the hydrolysis of $NaBH_4$. It is observed that in the presence of 10^{-1} M NaOH, H_2 generation ceases completely and can be initiated by adding the same molarity of HCl. However, it is observed that with each "on–off" cycle there is a gradual decrease in the hydrogen production. This can be explained by the "common ion effect" of NaCl produced during the neutralization reaction of NaOH with the externally added HCl. The following process happens in aqueous medium.

$$NaCl \leftrightarrow Na^{+} + Cl^{-} \quad \text{(i)}$$

$$NaBH_4 \leftrightarrow Na^{+} + BH_4^{-} \quad \text{(ii)}$$

With the successive addition of HCl, the concentration of NaCl increases in the reaction system which prevents further $NaBH_4$ hydrolysis, according to Le Chatelier's principle.

The effect of temperature on the hydrogen generation rate was further explored for sample B through the variation of temperature in the range of 283–313 K. Fig. 7a depicts the volume of H_2 production *versus* time. It is observed that the reaction temperature had a remarkable effect on the volume of H_2 generated. For a reaction temperature of 283 K, 353 ml of H_2 is produced, while 878 ml is produced at 313 K. Activation energy is an important parameter to study the kinetics of H_2 production. It can be calculated from the following Arrhenius equation:[54]

$$\ln k = \ln A - (E_a/RT)$$

where k is the reaction rate constant (mol min^{-1} g^{-1}), A is the pre-exponential factor, E_a is the activation energy (kJ mol^{-1}), T is

the absolute temperature in K, and R is the gas constant (8.314 J K^{-1} mol^{-1}). In Fig. 7b, ln k *versus* $1/T$ is plotted and E_a is found to be 22.01 kJ mol^{-1} for sample B. It may be noted here that E_a for our metal free CNDs is much lower than the popular costly metals during hydrolysis and even significantly comparable with some metal free catalysts, used in methanolysis of $NaBH_4$ (Table 2).

Conclusion

We report for the first time, an efficient metal-free and cheap CND catalyst for controlled hydrolysis of $NaBH_4$, that paves a way for on-board and on-demand H_2 production. CNDs were synthesized with negatively and positively charged functional groups by treating CA and CA with urea, respectively, using a domestic microwave oven. Negatively charged functional groups are futile, while positively charged functional groups felicitate the hydrolysis reaction, and the activity is highly dependent on the surface area. Reusability, conversion and true activity studies confirm the as-synthesized CNDs as a potential candidate in the practical field of H_2 production. The effect of temperature as well as the pH of the reaction medium were investigated. The activity was found to increase with temperature, and decrease with pH. Attractive and effective "on–off" control was observed just by varying the pH of the reaction medium. Interestingly, an activation energy of 22.01 kJ mol^{-1} is extracted from the temperature-dependent activity and the activation energy is much lower than that reported for other systems.

Acknowledgements

The author (SS) wishes to thank Ms. Shubhanwita Saha (Jadavpur University, Kolkata) and Dr. Sayantani Chall (Indian Institute of Chemical Biology, Kolkata) for many insightful discussions and acknowledges the financial support from University Grants Commission (UGC), the Government of India, through Dr. D. S. Kothari Postdoctoral Fellowship.

References

1 Z. Pu, I. S. Amiinu, X. Liu, M. Wang and S. Mu, *Nanoscale*, 2016, **8**, 17256.
2 S. R. Soltau, P. D. Dahlberg, J. Niklas, O. G. Poluektov, K. L. Mulfort and L. M. Utschig, *Chem. Sci.*, 2016, **7**, 7068.
3 D. Basu, S. Mazumder, J. Niklas, H. Baydoun, D. Wanniarachchi, X. Shi, R. J. Staples, O. Poluektov, H. B. Schlegel and C. N. Verani, *Chem. Sci.*, 2016, **7**, 3264.
4 S. C. Amendola, S. L. Sharp-Goldman, M. S. Janjua, N. C. Spencer, M. T. Kelly, P. J. Petillo and M. Binder, *Int. J. Hydrogen Energy*, 2000, **25**, 969.
5 M. Granovskii, I. Dincer and M. A. Rosen, *Int. J. Hydrogen Energy*, 2006, **31**, 337.
6 Z. Liu, B. Guoa, S. H. Chan, E. H. Tang and L. Hong, *J. Power Sources*, 2008, **176**, 306.
7 N. Jia, M. C. Lefebvre, J. Halfyard, Z. Qi and P. G. Pickup, *Electrochem. Solid-State Lett.*, 2000, **3**, 529.
8 P. Krishnan, T. H. Yang, W. Y. Lee and C. S. Kim, *J. Power Sources*, 2005, **143**, 17.
9 P. Costamagna and S. Srinivasan, *J. Power Sources*, 2001, **102**, 253.
10 M. T. Gencoglu and Z. Ural, *Int. J. Hydrogen Energy*, 2009, **34**, 5242.
11 B. Najafi, A. H. Mamaghani, A. Baricci, F. Rinaldi and A. Casalegno, *Int. J. Hydrogen Energy*, 2015, **40**, 1569.
12 P. Krishnan, K. L. Hsueh and S. D. Yim, *Appl. Catal., B*, 2007, **77**, 206.
13 Ö. Metin and S. Özkar, *Energy Fuels*, 2009, **23**, 3517.
14 R. Retnamma, A. Q. Novais and C. M. Rangel, *Int. J. Hydrogen Energy*, 2011, **36**, 9772.
15 S. Saha, V. Basak, A. Dasgupta, S. Ganguly, D. Banerjee and K. Kargupta, *Int. J. Hydrogen Energy*, 2014, **39**, 1156.
16 H. I. Schlesinger, H. C. Brown, A. E. Finholt, J. R. Gilbreath, H. R. Hoekstra and E. K. Hyde, *J. Am. Chem. Soc.*, 1953, **75**, 215.
17 P. Y. Olu, C. R. Barros, N. Job and M. Chatenet, *Electrocatalysis*, 2014, **5**, 288.
18 W. Chen, J. Ji, X. Feng, X. Duan, G. Qian, P. Li, X. Zhou, D. Chen and W. Yuan, *J. Am. Chem. Soc.*, 2014, **136**, 16736.
19 U. B. Demirci and F. Garin, *J. Alloys Compd.*, 2008, **463**, 107.
20 Y. Du, J. Su, W. Luo and G. Cheng, *ACS Appl. Mater. Interfaces*, 2015, **7**, 1031.
21 Z. Zhang, Z. H. Lu and X. Chen, *ACS Sustainable Chem. Eng.*, 2015, **3**, 1255.
22 J. C. Ingersoll, N. Mania, J. C. Thenmozhiyal and A. Muthaiah, *J. Power Sources*, 2007, **173**, 450.
23 Z. Wu, X. Mao, Q. Zi, R. Zhang, T. Dou and A. C. K. Yip, *J. Power Sources*, 2014, **268**, 596.
24 L. Yang, K. Wang, G. Du, W. Zhu, L. Cui, C. Zhang, X. Sun and A. M. Asiri, *Nanotechnology*, 2016, **27**, 475702.
25 J. Zhu, R. Li, W. Niu, Y. Wu and X. Gou, *Int. J. Hydrogen Energy*, 2013, **38**, 10864.
26 M. Paladini, V. Godinho, G. M. Arzac, M. C. J. Haro, A. M. Beltŕan and A. Ferńandez, *RSC Adv.*, 2016, **6**, 108611.
27 O. V. Netskina, A. M. Ozerova, O. V. Komova, D. I. Kochubey, V. V. Kanazhevskiy, A. V. Ishchenko and V. I. Simagina, *Top. Catal.*, 2016, **59**, 1431.
28 M. Zahmakıran and S. Özkar, *Nanoscale*, 2011, **3**, 3462.
29 Y. Li, X. Zhang, Q. Zhang, J. B. Zheng, N. Zhang, B. H. Chena and K. J. Smith, *RSC Adv.*, 2016, **6**, 29371.
30 A. Chinnappan, R. Appiah-Ntiamoah, W. J. Chung and H. Kim, *Int. J. Hydrogen Energy*, 2016, **41**, 14491.
31 S. Qu, X. Wang, Q. Lu, X. Liu and L. Wang, *Angew. Chem., Int. Ed.*, 2012, **51**, 12215.
32 P. M. Schaber, J. Colson, S. Higgins, D. Thielen, B. Anspach and J. Brauer, *Thermochim. Acta*, 2014, **424**, 131.
33 H. K. Sadhanala, J. Khatei and K. K. Nanda, *RSC Adv.*, 2014, **4**, 11481.
34 R. Purbia and S. Paria, *Biosens. Bioelectron.*, 2016, **79**, 467.
35 D. B. Mawhinney and J. T. Yates Jr, *Carbon*, 2001, **39**, 1167.
36 D. B. Clarke, D. K. Lee, M. J. Sandoval and A. T. Bell, *J. Catal.*, 1994, **150**, 81.
37 J. Bak and S. Clausen, *Meas. Sci. Technol.*, 2002, **13**, 150.
38 Y. Li, Y. Zhao, H. Cheng, Y. Hu, G. Shi, L. Dai and L. Qu, *J. Am. Chem. Soc.*, 2012, **134**, 15.

39 R. Zhang and W. Chen, *Biosens. Bioelectron.*, 2014, **55**, 83.
40 Z. Yang, M. Xu, Y. Liu, F. He, F. Gao, Y. Su, H. Wei and Y. Zhang, *Nanoscale*, 2014, **6**, 1890.
41 S. Liu, J. Tian, L. Wang, Y. Zhang, X. Qin, Y. Luo, A. M. Asiri, A. O. Al-Youbi and X. Sun, *Adv. Mater.*, 2012, **24**, 2037.
42 X. Xiang, E. Liu, Z. Huang, H. Shen, Y. Tian, C. Xiao, J. Yang and Z. Mao, *J. Solid State Electrochem.*, 2011, **15**, 2667.
43 S. J. Kang, T. Mori, S. Narizuka, W. Wilcke and H. C. Kim, *Nat. Commun.*, 2014, **5**, 3937.
44 F. Lux, E. J. Samuelsen and E. T. Kang, *Synth. Met.*, 1995, **69**, 167.
45 L. Shi, Y. Wang, Z. Chu, Y. Yin, D. Jiang, J. Luo, S. Ding and W. Jin, *J. Mater. Chem. B*, 2017, **5**, 1073.
46 D. B. Shinde and V. K. Pillai, *Chem.–Eur. J.*, 2012, **18**, 12522.
47 N. Sahiner and F. Seven, *Fuel Process. Technol.*, 2015, **132**, 1.
48 N. Sahiner, T. Turhan and L. A. Lyon, *Energy*, 2014, **66**, 256.
49 J. Zhao, H. Ma and J. Chen, *Int. J. Hydrogen Energy*, 2007, **32**, 4711.
50 Y. Chen, Y. Shi and Y. Wang, *Int. J. Energy Res.*, 2015, **39**, 634.
51 H. Jin, J. Wang, D. Su, Z. Wei, Z. Pang and Y. Wang, *J. Am. Chem. Soc.*, 2015, **137**, 2688.
52 N. Sahiner and A. O. Yasar, *Ind. Eng. Chem. Res.*, 2016, **55**, 11245.
53 P. Barack, S. E. Dann and K. G. U. Wijayantha, *Energy Sci. Eng.*, 2015, **3**, 174.
54 A. Chinnappan, W. J. Chung and H. Kim, *J. Mater. Chem. A*, 2015, **3**, 22960.
55 S. C. Amendola, S. L. Sharp-Goldman, M. S. Janjua, M. T. Kelly, P. J. Petillo and M. Binder, *J. Power Sources*, 2000, **85**, 186.
56 D. Hua, Y. Hanxi, A. Xinping and C. Chuansin, *Int. J. Hydrogen Energy*, 2003, **28**, 1095.
57 S. Özkar and M. Zahmakıran, *J. Alloys Compd.*, 2005, **404–406**, 728.
58 H. Cai, L. Liu, Q. Chen, P. Lu and J. Dong, *Energy*, 2016, **99**, 129.
59 M. Tang, F. Xia, C. Gao and H. Qiu, *Int. J. Hydrogen Energy*, 2016, **41**, 13058.
60 N. Sahiner and S. B. Sengel, *J. Power Sources*, 2016, **336**, 27.
61 N. Sahiner, A. O. Yasar and N. Aktas, *Renewable Energy*, 2017, **101**, 1005.
62 D. Xu, Y. Zhang, F. Cheng and L. Zhao, *Fuel*, 2014, **134**, 257.
63 N. Sahiner, A. O. Yasar and N. Aktas, *Int. J. Hydrogen Energy*, 2016, **41**, 20562.
64 N. Sahiner and S. Demirci, *Int. J. Energy Res.*, 2016, DOI: 10.1002/er.3679.